tion of protein mixtures (*47*) or polystyrene standards (*48*) can be achieved in a very short time (Fig. 10). The high speed of these separations indicates that these monoliths can be used for real-time process control and the design of smaller units with the very high throughput required for industrial separations, fast diagnostics, sensors, and many other applications.

Although much remains to be done in studies of advanced macroporous polymers, recent achievements in the preparation of both polymer beads and monoliths should open new avenues for the preparation of supports and separation media with exactly tailored properties.

REFERENCES AND NOTES

1. R. B. Merrifield, *J. Am. Chem. Soc.* **85**, 2149 (1963).
2. E. Bayer and W. Rapp, in *Poly(ethylene glycol) Chemistry: Biotechnical and Biomedical Applications*, J. Milton Harris, Ed. (Plenum, New York, 1992), pp. 325–345.
3. J. Seidl, J. Malinsky, K. Dusek, W. Heitz, *Adv. Polym. Sci.* **5**, 11 (1967); A. Guyot and M. Bartholin, *Prog. Polym. Sci.* **8**, 277 (1982); K. A. Kun and R. Kunin, *J. Polym. Sci. A* **6**, 2689 (1968); W. L. Sederel and G. J. DeJong, *J. Appl. Polym. Sci.* **17**, 2835 (1973).
4. J. M. J. Fréchet, *Makromol. Chem. Macromol. Symp.* **70-71**, 289 (1993).
5. K. K. Unger, *Packings and Stationary Phases in Chromatographic Techniques* (Dekker, New York, 1990).
6. J. Porath and P. Flodin, *Nature* **183**, 1657 (1959).
7. K. Mosbach, Ed., *Methods in Enzymology* (Academic Press, New York, 1976).
8. R. G. Gilbert, *Emulsion Polymerization: A Mechanistic Approach* (Academic Press, London, 1995).
9. K. E. J. Barrett, *Dispersion Polymerization in Organic Media* (Wiley, New York, 1975); C. K. Ober, *Makromol. Chem. Macromol. Symp.* **35-36**, 87 (1990); M. D. Croucher and M. A. Winnik, in *Future Directions in Polymer Colloids*, M. S. El-Aasser and R. M. Fitch, Eds. (NATO ASI Ser. E 138, Nijhoff, Dordrecht, 1987), pp. 209–227; Y. L. Hsiao, E. E. Maury, J. M. Desimone, S. Mawson, K. P. Johnson, *Macromolecules* **28**, 8159 (1995).
10. F. M. Winnik and C. K. Ober, *Eur. Polym. J.* **23**, 617 (1987); D. Horak, F. Svec, J. M. J. Fréchet, *J. Polym. Sci. Polym. Chem. Ed.* **33**, 2961 (1995).
11. German patents 254,672 and 255,129, which describe the preparation of synthetic polybutadiene and polyisoprene rubber, respectively, by a simple process similar to suspension polymerization, were issued on 26 January and 13 March 1912 to Farbenfabriken Bayer, Elberfeld, Germany.
12. B. W. Brooks, *Makromol. Chem. Macromol. Symp.* **35-36**, 121 (1990); H. G. Yuan, G. Kalfas, W. H. Ray, *J. Macromol. Sci. C* **31**, 215 (1991).
13. J. M. J. Fréchet, *Tetrahedron* **37**, 663 (1881); K. Smith, Ed., *Solid Supports and Catalysts in Organic Synthesis* (Horwood, Chichester, UK, 1992); N. K. Terrett, M. Gardner, D. W. Gordon, R. J. Kobylecki, J. Steele, *Tetrahedron* **51**, 8135 (1995).
14. E. Ruckenstein and L. Hong, *Polymer* **36**, 2857 (1995).
15. S. Omi, K. Katami, A. Yamamoto, M. Iso, *J. Appl. Polym. Sci.* **51**, 1 (1994); S. Omi, K. Katami, T. Taguchi, K. Kaneko, M. Iso, *ibid.* **57**, 1013 (1995).
16. A. Kostner and M. Mandel, *Enzymologia* **44**, 191 (1976); W. K. Rhim, M. T. Hyson, S. K. Chung, M. S. Colvin, M. Chang, *NASA Tech. Briefs* (September 1989), p. 98; P. Schummer and K. H. Tebel, *Ger. Chem. Eng.* **5**, 209 (1982).
17. J. H. Kim, F. D. Sudol, M. S. El-Aasser, J. W. Wanderhoff, D. M. Kornfield, *Chem. Eng. Sci.* **43**, 2025 (1988); J. W. Wanderhoff *et al.*, *J. Dispersion Sci. Technol.* **5**, 231 (1984).
18. J. Ugelstad *et al.*, *Prog. Polym. Sci.* **17**, 87 (1992).
19. Q. C. Wang, K. Hosoya, F. Svec, J. M. J. Fréchet, *Anal. Chem.* **64**, 1232 (1992); Q. C. Wang, F. Svec, J. M. J. Fréchet, *J. Polym. Sci. A* **32**, 2577 (1994).
20. K. Lewandowski, F. Svec, J. M. J. Fréchet, *J. Liq. Chromatogr.*, in press; V. Smigol, F. Svec, J. M. J. Fréchet, *ibid.* **17**, 259 (1994).
21. K. Ogino, H. Sato, K. Tsuchiya, H. Suzuki, S. Moriguchi, *J. Chromatogr. A* **699**, 59 (1995); *ibid.*, p. 67.
22. C. Cheng, F. J. Micale, J. W. Wanderhoff, M. S. El-Aasser, *J. Polym. Sci. Polym. Chem. Ed.* **30**, 235 (1992); *ibid.*, p. 245.
23. P. Hodge and D. C. Sherrington, Eds., *Syntheses and Separations Using Functional Polymers* (Wiley, New York, 1989).
24. T. C. Pinkerton, *J. Chromatogr.* **544**, 13 (1991); J. Haginaka, *Trends Anal. Chem.* **10**, 17 (1991); D. J. Anderson, *Anal. Chem.* **65**, 434R (1993).
25. K. Hosoya *et al.*, *J. Chromatogr. A* **690**, 21 (1995).
26. K. Hosoya *et al.*, *Anal. Chem.* **67**, 1907 (1995).
27. K. Hosoya *et al.*, *J. Chromatogr. A* **666**, 449 (1994).
28. J. C. Moore, *J. Polym. Sci. A* **2**, 842 (1962).
29. V. Smigol, F. Svec, J. M. J. Fréchet, *Macromolecules* **26**, 5615 (1993).
30. ———, *Anal. Chem.* **66**, 2129 (1994); *ibid.*, p. 4308.
31. L. R. Snyder and J. J. Kirkland, *Introduction to Modern Liquid Chromatography* (Wiley, New York, 1979).
32. P. S. J. Cheetham, in *Handbook of Enzyme Technology*, A. Wiseman, Ed. (Horwood, Chichester, UK, 1985), pp. 54–142.
33. D. Lee, *J. Chromatogr.* **443**, 143 (1988).
34. A. Nir and L. Pismen, *Chem. Eng. Sci.* **32**, 35 (1977).
35. F. E. Regnier, *Nature* **350**, 634 (1991); N. B. Afeyan *et al.*, *J. Chromatogr.* **519**, 1 (1990).
36. A. E. Rodrigues, Z. P. Lu, J. M. Loureiro, G. Carta, *J. Chromatogr.* **653**, 93 (1993); A. I. Liapis, *Math. Modeling Sci. Comput.* **1**, 397 (1993).
37. D. K. Roper and E. N. Lightfoot, *J. Chromatogr. A* **702**, 3 (1995).
38. J. L. Manganaro and B. S. Goldberg, *Biotechnol. Prog.* **9**, 285 (1993); D. F. Hagen, C. G. Markell, G. A. Smitt, D. D. Blevins, *Anal. Chim. Acta* **236**, 157 (1990).
39. T. B. Tennikova and F. Svec, *J. Chromatogr.* **646**, 279 (1993).
40. J. F. Kennedy and M. Paterson, *Polym. Int.* **32**, 71 (1993).
41. Y. Yang, A. Velayudhan, C. M. Ladish, M. R. Ladish, *J. Chromatogr.* **598**, 169 (1992).
42. K. Nakazano, J. Mohammad, S. Hjertén, *Chromatographia* **39**, 655 (1994).
43. F. Svec and J. M. J. Fréchet, *Anal. Chem.* **64**, 820 (1992).
44. ———, *Chem. Mater.* **6**, 707 (1995).
45. M. Petro, F. Svec, J. M. J. Fréchet, *Biotechnol. Bioeng.* **49**, 355 (1996).
46. J. J. Van Deemter, F. J. Zuiderweg, A. Klinkenberg, *Chem. Eng. Sci.* **5**, 271 (1956).
47. Q. C. Wang, F. Svec, J. M. J. Fréchet, *Anal. Chem.* **65**, 2243 (1993).
48. M. Petro, F. Svec, I. Gitsov, J. M. J. Fréchet, *ibid.* **68**, 315 (1996).

49. Supported in part by NIH grants GM 48364-02 and GM 44885-05.

RESEARCH ARTICLE

Transcription Processivity: Protein-DNA Interactions Holding Together the Elongation Complex

Evgeny Nudler,* Ekaterina Avetissova, Vadim Markovtsov, Alex Goldfarb

The elongation of RNA chains during transcription occurs in a ternary complex containing RNA polymerase (RNAP), DNA template, and nascent RNA. It is shown here that elongating RNAP from *Escherichia coli* can switch DNA templates by means of end-to-end transposition without loss of the transcript. After the switch, transcription continues on the new template. With the use of defined short DNA fragments as switching templates, RNAP-DNA interactions were dissected into two spatially distinct components, each contributing to the stability of the elongating complex. The front (F) interaction occurs ahead of the growing end of RNA. This interaction is non-ionic and requires 7 to 9 base pairs of intact DNA duplex. The rear (R) interaction is ionic and requires approximately six nucleotides of the template DNA strand behind the active site and one nucleotide ahead of it. The nontemplate strand is not involved. With the use of protein-DNA crosslinking, the F interaction was mapped to the conserved zinc finger motif in the NH_2-terminus of the β′ subunit and the R interaction, to the COOH-terminal catalytic domain of the β subunit. Mutational disruption of the zinc finger selectively destroyed the F interaction and produced a salt-sensitive ternary complex with diminished processivity. A model of the ternary complex is proposed here that suggests that trilateral contacts in the active center maintain the nonprocessive complex, whereas a front-end domain including the zinc finger ensures processivity.

In the advancing elongation complex, RNAP combines two contradictory biochemical features: (i) exceptional stability for dissociation and (ii) the ability to easily translocate along DNA. Thus, elongating RNAP simultaneously behaves as a strong

DNA binding protein and as a protein with no affinity for particular DNA sites. The combination of these features ensures the processivity of RNAP. Both of these features can be modulated by DNA-encoded signals and protein factors that cause termination, antitermination, and pausing (*1–3*).

To explain elongation, one must account for the fact that in initiation RNAP behaves as a site-specific DNA binding protein that is anchored to the promoter site. During the transition from initiation to elongation, RNAP must undergo a fundamental change in the nature of interactions that hold the complex together. When the complex leaves the promoter, it acquires salt resistance (*4*). Thus, the newly established elongation-specific interactions must be of a non-ionic nature. Here, we identified structural elements, both in DNA and RNAP, that participate in the maintenance of the elongation complex, with particular emphasis given to the distinction between ionic and non-ionic interactions.

End-to-end template switching. In the course of in vitro transcription studies, we found that elongating RNAP could switch to a new DNA fragment when it reached the end of template DNA (Fig. 1). For these experiments, we used RNAP with six extra His residues fused to the COOH-terminus of the β′ subunit. The enzyme adsorbs to Ni^{2+}-agarose beads by means of the His^6 tag. This allows assays to be performed in the solid phase, which in turn permits the rapid exchange of reaction components by centrifugation and washing of the beads. With the use of this technique, His^6-tagged RNAP can be walked along the template in controlled steps (*5, 6*). In the experiment shown in Fig. 1, RNAP was walked to position +34 of the promoter DNA fragment (primary template). The washed complex was then allowed to continue polymerization ("chase") to the end of the primary template by addition of four nucleoside triphosphates (NTPs) to yield a 49-nucleotide (nt) runoff RNA (lane 2). Both the runoff transcript and the primary template DNA dissociated from RNAP after washing with buffer with a high salt concentration (0.5 M KCl; "high-salt buffer") because they could not be recovered from the beads (lane 3). However, when the chase was performed in the presence of an excess of a 24-bp double-stranded oligonucleotide (secondary template), a longer runoff product was formed (lane 4), whose size suggested that transcription had switched to the new template.

To document the switchover event in detail, we designed a protocol that would stall the elongating complex within the secondary template. The secondary template carried the first adenine residue six nucleotides (nt) away from the 3′ terminus of the bottom strand, whereas the top strand carried an adenine at the 3′ terminus (Fig. 1). At the same time, the primary template had no adenine residues downstream from position +34. Thus, by withholding uridine triphosphate (UTP) from the chase reaction (the "ACG" chase), the switchover synthesis was restricted to the bottom strand of the secondary template. This yielded a 55-nt switchover transcript (49 + 6 = 55), along with the 49-nt runoff RNA that apparently represented an attempt of the complex to switch to the wrong end of the secondary template (lane 5).

When the 55-nt switchover complex was washed with high-salt buffer, the primary template was lost. Polynucleotide kinase labeling of the washed +55 complex demonstrated that the primary template was replaced by the secondary template (lane 6). The switch- over complex could be walked farther down the secondary template in accordance with its nucleotide sequence. Each walking step yielded a transcript indistinguishable from the one obtained on the control template, which represents a fusion of the primary and secondary templates. Trace amounts of the 34-nt transcript and of the primary template present in every chase reaction represent the arrested elongation complex formed at position +34. Here it serves as an internal control that allows us to quantify the amount of the ternary complex material in the samples.

Template requirements for the ternary complex. The template switching phenomenon provides a powerful system to study RNAP-DNA interactions because the template region normally protected by RNAP can be changed to determine the requirements for the stability of the complex. We next assessed the differences of single- and double-stranded templates. For this, we have used the symbols "t" and "n" for the template and nontemplate strands, respectively, followed by the numerical identification of the oligonucleotide.

The switchover (represented by the 55-nt transcript) occurred both with the n1/t1 (double-stranded) and with the t1 (single-stranded) secondary template (Fig. 2). On the t1 template, however, the switchover was less than 100% accurate, as reflected by the appearance of minor products 54 nt and 53 nt long. We attribute this effect to RNAP skipping 1 or 2 nt during the jump. On both types of template, the washed switchover complex could be immediately chased into the 58-nt product by addition of adenosine triphosphate (ATP) and UTP. After a 30-min incubation at 37°C, the complex on the n1/t1 template was still able to be chased, whereas the complex on the t1 template lost activity by approximately 30%, as reflected by the residual 55-nt RNA. Control experiments showed that this inactivation was the result of dissociation rather than elongation arrest. Thus, at low salt concentration, the ternary complex on the single-stranded template is less stable than on the double-stranded DNA.

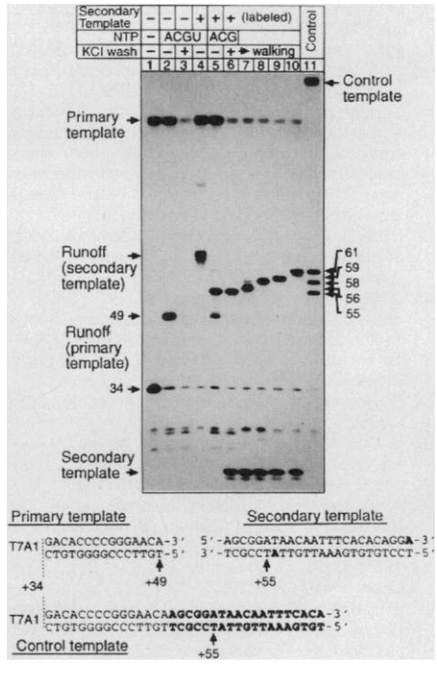

Fig. 1. End-to-end template switching. The autoradiogram shows RNA products and end-labeled DNA template fragments recovered from aliquots of a single transcription reaction using immobilized RNAP (*22*). A start-up ternary complex with 12-meric transcript was ^{32}P-labeled in the RNA in position +12C and in the DNA termini with polynucleotide kinase so that the specific radioactivity of both components was about the same. The complex was then walked to position +34C (lane 1), washed, and chased with the indicated sets of NTPs in the absence (lanes 2 and 3) or in the presence (lanes 4 through 6) of the secondary template. Where indicated, the complexes were washed with high-salt buffer (lanes 3 and 6). The secondary template in the high salt–washed +55A switchover complex (lane 6) was end-labeled with polynucleotide kinase, and the complex was then walked to positions +56T, +58A, +59C, and +61A with subsets of NTPs (lanes 7 through 10). Lane 11 presents a mixture of analogous reactions performed on the end-labeled control template to yield complexes +55A, +58A, and +61A. The structure of the three DNA templates is shown in the bottom. The primary and the control templates start with the T7A1 promoter sequence (*24*). The template elements discussed in the text are in bold. The arrows designate principal transcripts and show their endpoints on the template sequence.

The authors are in the Public Health Research Institute, New York, NY 10016, USA.

*To whom correspondence should be addressed.

The difference between the double- and single-stranded templates became obvious when the switchover complex was briefly exposed to high concentrations of salt: the former remained 100% intact, whereas the latter fell apart (Fig. 2). The residual runoff and arrested complexes (represented by the 49-nt and 34-nt RNA species) were salt-sensitive and salt-resistant, respectively. Finally, the switchover complex on the t1 template could be converted to salt resistance by addition of the n1 nontemplate strand. These results indicate that the RNAP-DNA interactions can be divided into two categories: salt-resistant and salt-sensitive. The salt-resistant interactions require the secondary template to be double-stranded.

To determine the minimal template parameters required for the salt-resistant complex, we prepared a series of secondary templates (Fig. 3). In each case, the half-life of the switchover complex was determined at high and low salt concentrations. Of the secondary templates tested, only n3/t1 and n3/t2 rendered the complex salt-resistant. The salt-resistant complex required no more than 9 bp of DNA duplex from +2 to +11 nt relative to the 3′ terminus of RNA. Beyond +11, no DNA was required (line 7), whereas the intact duplex at positions +10 and +11 was essential. Moving the 9-bp duplex area away from the RNA 3′ terminus led to a destabilization of the complex. Thus, the 9-bp duplex area ahead of the RNA terminus defines the site of RNAP responsible for the salt-resistant interactions.

An additional requirement for the salt-stable complex was the presence of about 6 nt of single-stranded template DNA upstream from the RNA end (Fig. 3A, lines 9 and 10). These experiments define the minimal template required for the salt stability (represented by fragment n3/t2) as a 17-nt, partially single-stranded DNA positioned in the ternary complex so that the first 6 nt have been transcribed and the double-stranded template is confined to the nine distal positions.

The salt-sensitive component of the RNAP interaction with the minimal tem-

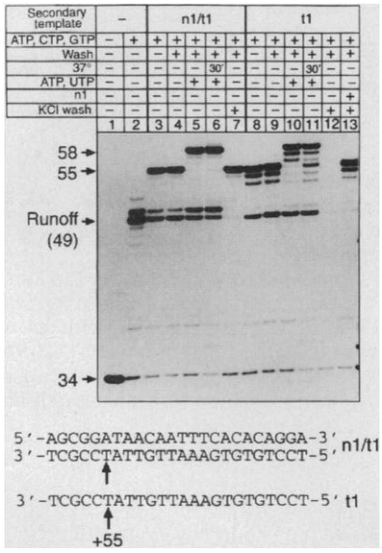

Fig. 2. Comparison of the switchover complex on double- and single-stranded DNA. The +34 complex was prepared, and the switchover reaction performed, as in Fig. 1 under the indicated conditions. The switchover occurred both with the n1/t1 (lane 3) and with the t1 (lane 8) secondary template. The washed switchover complex (lanes 4 and 9) could be immediately chased into the 58-nt product by addition of ATP and UTP (lanes 5 and 10). After a 30-min incubation at 37°C, the complex on the n1/t1 template was still able to be chased (lane 6), whereas the complex on the t1 template lost activity by approximately 30% (lane 11). At high salt, the switchover complex on the double-stranded template remained intact (lane 7), whereas on the single-stranded template, it fell apart (lane 12). The switchover complex on the t1 template could be converted to salt resistance by addition of the n1 nontemplate strand (lane 13).

Fig. 3. Determination of the minimal template parameters required for ternary complex stability. (**A**) Summary table. We determined the half-lives of the complexes by counting the radioactivity in the bands using Instant imager (Packard). For each complex with a half-life more than 1 min and less than 120 min, 10 to 15 time points were taken. In all cases, the decay followed first-order kinetics. Stability of the duplexes at +24°C at low salt was monitored by retention of end-labeled oligonucleotides. The salt-resistant complex required no more than 9 bp of DNA duplex from +2 to +11 nt relative to the 3′ terminus of RNA (lines 4 and 7). The intact duplex at positions +10 and +11 was essential (lines 3 and 8). Moving the 9-bp duplex area away from the RNA 3′ terminus led to a destabilization of the complex (lines 5 and 6). Lines 9 and 10 show the presence of about 6 nt of single-stranded template DNA upstream from the RNA end. Line 7 shows fragment n3/t2; lines 2 and 11 show the double-stranded region. (**B**) A representative experiment for the 20-min time point. Experimental details are as in Fig. 1. Of the secondary templates tested, only n3/t1 (lane 8) and n3/t2 (lane 14) rendered the complex salt-resistant.

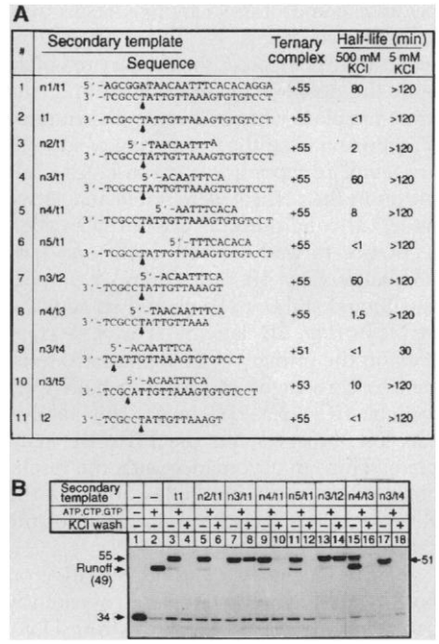

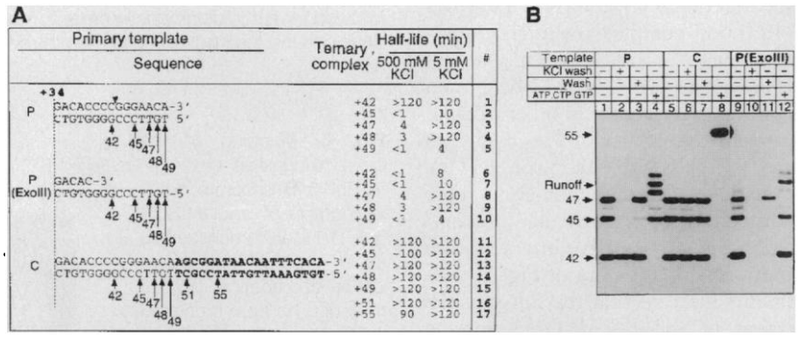

Fig. 4. Delineation of the salt-sensitive upstream interaction. The cumulative table (**A**) and a representative experiment (**B**) (20-min time point) are presented. The primary (P) and the control (C) templates are the same as in Fig. 1. The complexes on the ExoIII-trimmed primary template [P(ExoIII)] were prepared with the combination of walking and nuclease digestion (*26*). The +20 ternary complex prepared by standard walking was exposed to ExoIII. Under these conditions, degradation of the nontemplate strand stops 19 nt ahead of the RNA 3′ terminus (*6*), which we confirmed by sequencing controls for more than 90% of the active complexes. After removal of ExoIII, the complex was treated with Sma I restriction endonuclease [arrowhead in (A)] to cleave the residual duplex at +42. The complex was then walked to the positions desired, as indicated by the upward-pointing arrows. In the data shown here, three DNA templates were compared: the primary template with the double-stranded (blunt) end [P; (A), lines 1 through 5; (B), lanes 1 through 4], the same template with a 10-nt single-stranded 5′ overhang [P(ExoIII); (A), lines 6 through 10; (B), lanes 9 through 12], and the fused primary-secondary template serving as a control [C; (A), lines 11 through 17; (B), lanes 5 through 8].

plate did not require the double-stranded region but was dependent on the presence of at least 4 nt of template strand DNA upstream from the RNA 3′ terminus. To further analyze the salt-sensitive interactions, we studied the ternary complexes positioned near the end of the primary template so that the front (F) salt-resistant contacts involving the DNA duplex could not exist. The half-lives of the complexes are summarized in Fig. 4A. A representative single-time-point experiment for three complexes carrying transcripts 42, 45, and 47 nt long (that is, stopped 7, 4, and 2 nt before the end of the template, respectively) is shown in Fig. 4B. Three DNA templates were compared: the primary template with the double-stranded (blunt) end, the same template with a 10-nt single-stranded 5′ overhang , and the fused primary-secondary template serving as a control. All complexes in the control were stable and active under all conditions, as evident from their resistance to washing with high- and low-salt buffer (Fig. 4B, lanes 6 and 7, respectively) and ability to be chased on addition of NTPs (Fig. 4B, lane 8). The +42 complex on the primary (P) template was resistant to both high- and low-salt buffer and was able to be chased (lane 4). This stability was lost, however, on the P(ExoIII) template. Thus, in accordance with the results above, at least a 7-bp duplex ahead of the RNA terminus must be maintained for the salt-resistant contacts.

The +47 complex was salt-sensitive on both P and P(ExoIII) templates, apparently as a result of the absence of the front DNA duplex. However, it was perfectly stable and active at low salt concentrations. The same was true for the +48 complex. However, the +49 runoff complex was highly unstable under low salt conditions. Thus, at least 1 nt of template DNA should be present ahead of the active center in order to maintain salt-sensitive contacts. The +45 complex was much less stable than the +47 and +48 complexes. This phenomenon represents the effect of a particular sequence context on the salt-sensitive interaction. In combination with the data of Fig. 3, these experiments indicate that the salt-sensitive component of the RNAP-DNA interactions involves the unpaired template strand of DNA and is confined to the segment of about 6 nt from −5 to +1 relative to the RNA 3′ terminus.

Mapping of template contact sites in RNAP. The minimal DNA template established above can be used as a probe for the mapping of protein sites involved in the maintenance of the ternary complex. To this end, we introduced 5-iododeoxyuridine, a derivative of thymidine that is able to be cross-linked, into defined positions of the secondary template (Fig. 5A). The reagent was placed into the template strand of the double-stranded DNA oligonucleotides in positions −3, +1, and +6 relative to the RNA 3′ terminus, so that it would mark the three principal localities envisaged in the complex—that is, the rear area of salt-sensitive DNA interaction, the active center, and the front area where the salt-resistant interaction occurs. The fragment derivatized in the +6 position was also used in the single-stranded form. The derivatized templates appeared only in the switchover (+55) but not in the +34 complexes (Fig. 5B), which illustrates that the binding was specific.

After brief exposure to ultraviolet light (UV) to induce crosslinking, the complexes were denatured and subjected to SDS–polyacrylamide gel electrophorhesis (SDS-PAGE) followed by autoradiography in order to visualize RNAP subunits carrying the cross-linked radiolabeled DNA (Fig. 5C). Only the samples containing the switchover complex produced radioactive bands.

In the switchover complex on the double-stranded template, the −3 and +1 probes crosslinked predominantly to the β subunit, whereas the +6 probe crosslinked to both β and β′ in approximately equal proportions (Fig. 5C). The β′ subunit crosslinking requires double-stranded DNA as it is diminished in size on the single-stranded template. In conjunction with our earlier results, this observation indicates that a site of the β′ subunit participates exclusively in the front interaction involv-

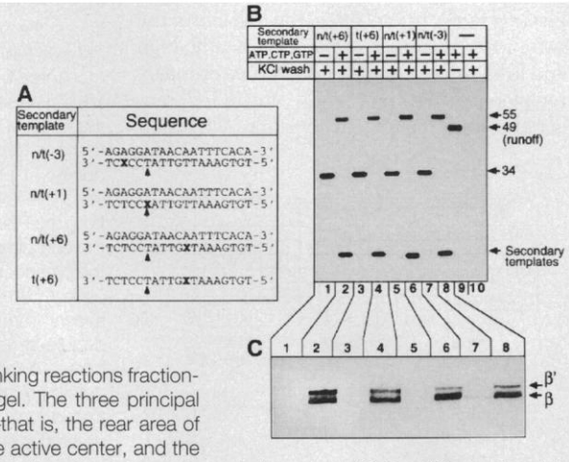

Fig. 5. Crosslinking of the secondary template probes to RNAP subunits (*27*). (**A**) Configurations of the secondary template carrying the 5-iododeoxyuridine residue that was able to be cross-linked. The upward-pointing arrows indicate the endpoint of RNA in the +55 complex. (**B**) Autoradiogram showing RNA products in each +55 complex, obtained by chasing a +34 starting complex. The DNA template (bottom) oligonucleotide was end-labeled with polynucleotide kinase. (**C**) Autoradiogram showing the material from the crosslinking reactions fractionated on a 4% polyacrylamide-SDS gel. The three principal localities envisaged in the complex—that is, the rear area of the salt-sensitive DNA interaction, the active center, and the front area where the salt-resistant interaction occurs—are shown in lanes 1 and 2, 5 and 6, and 7 and 8, respectively, in (B) and (C). The fragment derivatized in the +6 position was also used in the single-stranded form (lanes 3 and 4). Lanes 9 and 10 in (B) show a control without a secondary template. After brief exposure to UV to induce crosslinking, the complexes were denatured and subjected to SDS-PAGE followed by autoradiography in order to visualize RNAP subunits carrying the crosslinked radiolabeled DNA (C). Only the samples containing the switchover complex (lanes 2, 4, 6, and 8) produced radioactive bands.

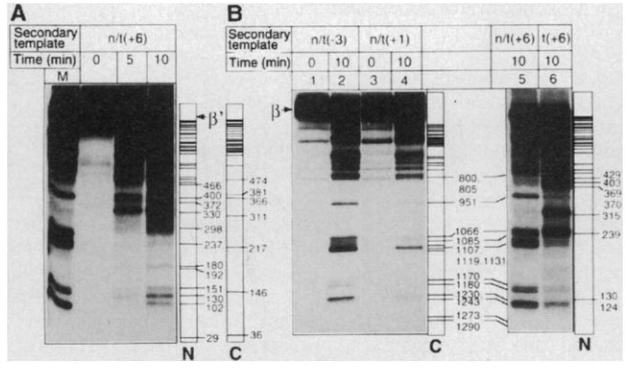

Fig. 6. Mapping of the crosslinking sites in the β′ (**A**) and β (**B**) subunits. Autoradiograms of gradient SDS gels (10 to 20% acrylamide) show products of partial CNBr degradation (*25*) of the subunits from irradiated +55 switchover complexes of Fig. 5C. As reference markers, the degradation products of the β subunit labeled with the same tag near His^{1237} are shown in lane M. The bar columns on the right of the panels show the theoretical patterns of the NH_2-terminal (N) and COOH-terminal (C) families of Met fragments, with the numbers indicating the positions of Met residues in the polypeptide chains. For discussion of the mapping principle, see (*25*). In (B), with the double-stranded template the degradation pattern is the same regardless of whether the crosslink came from the −3, +1, or +6 position (lanes 2, 4, and 5, respectively). The fragmentation pattern is identical to that of the β subunit carrying a unique radioactive ATP crosslinked to His^{1237}.

ing the DNA duplex, whereas the β subunit is involved in the rear ionic interactions.

To map the protein sites marked by the crosslinks, we excised the radioactive protein bands from the SDS gel (Fig. 5C) and subjected them to limited degradation with CNBr, which cleaves polypeptide chains next to Met residues. The cleavage products were fractionated by SDS-PAGE and visualized by autoradiography (Fig. 6). Under the single-hit conditions of limited degradation, two families of nested fragments were generated, which represent the COOH- and the NH_2-terminal products of each cleavage. If the cross-linked radioactive adduct is situated close to one of the termini, only one of the two fragment families will be seen on the gel autoradiogram, permitting unequivocal localization of the crosslink site between two adjacent Met residues (*7*).

Figure 6A illustrates the degradation of the radiotagged β' subunit from the n/t(+6) complex (Fig. 5C, lane 2) exposed to CNBr for 0, 5, and 10 min. For size markers, we used the known CNBr fragmentation pattern of the β subunit uniquely labeled with the same tag at His^{1237} (*7*). The experimental pattern of the β′ subunit degradation matches that of the theoretical NH_2-terminal family, and the shortest radioactive fragment is that of Met^{102}. Thus, the crosslink generated by the double-stranded +6 probe is situated between Met^{30} and Met^{102} near the NH_2-terminus of the β′ subunit.

Figure 6B presents the results of CNBr fragmentation of the radioactive β subunit obtained by UV crosslinking of the n/t(-3), n/t(+1), n/t(+6), and t(+6) probes. With the double-stranded template, the degradation pattern is the same regardless of whether the crosslink came from the −3, +1, or + 6 position. The fragmentation pattern matches the theoretical COOH-terminal family and is identical to that of the β subunit carrying the radioactive tag crosslinked to His^{1237}. The shortest radioactive band seen on the gel is that of $Met^{1230/1234}$. Thus, on the double-stranded template, the crosslink from the −3, +1, or +6 probe goes into the same segment near the COOH-terminus of the β subunit between Met^{1230} and Met^{1273}.

Inspection of the lane of Fig. 6B farthest to the right reveals that it contains a combination of both theoretically expected degradation patterns of the β subunit. The weaker pattern matches that of the COOH-terminal family and the stronger one fits that of the NH_2-terminal family starting with the fragment Met^{239}. The preceding theoretical NH_2-terminal fragments $Met^{124/130}$ are not seen in the stronger pattern. From this, we conclude that in the case of the single-stranded +6 probe, the crosslink goes preferentially into the NH_2-terminal part of the β subunit between Met^{130} and Met^{239}. A minor fraction of the crosslink goes into the COOH-terminus of β.

The role of a zinc finger in the salt-resistant interaction. These results suggest that the NH_2-terminal region of the β′ subunit participates in the salt-resistant interaction with double-stranded DNA ahead of the active center. Inspection of the amino acid sequence in this region reveals a motif with characteristically positioned Cys

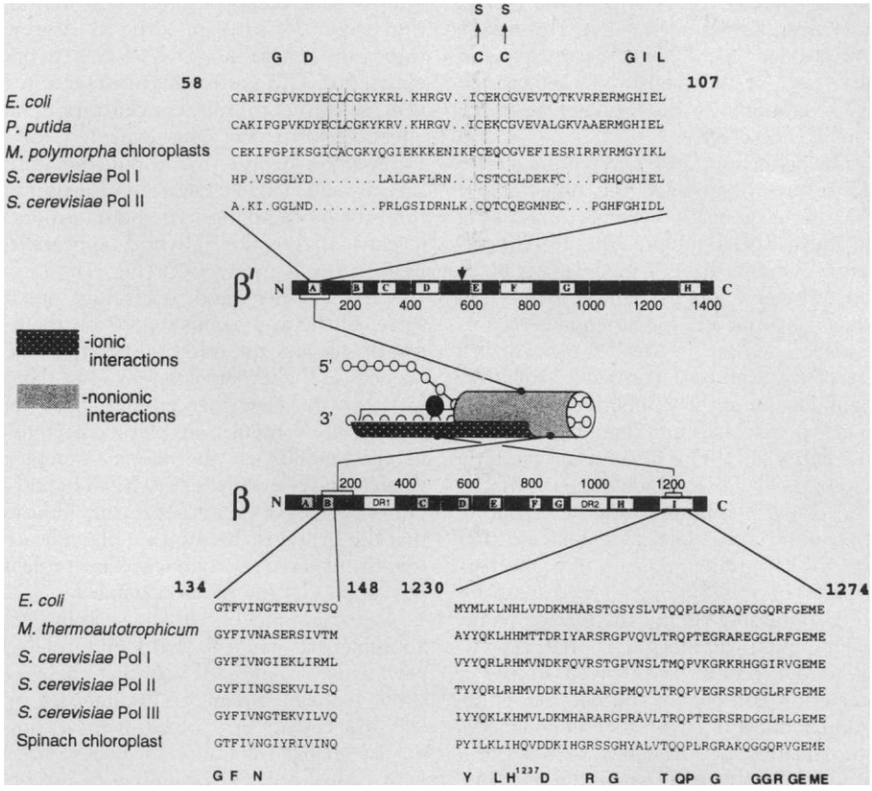

Fig. 7. Map of RNAP-DNA interactions in the ternary complex. The heavy bars represent the β′ and β polypeptides with evolutionarily conserved regions shaded in gray and designated by capital letters (*28*). DR1 and DR2 designate the dispensable regions that separate three principal domains in the β subunit (*13*). The downward-pointing arrow indicates the site of the β′ subunit sequence split in chloroplasts (*29*). Regions identified by DNA crosslinking are expanded into amino acid sequences, which are aligned with homologous regions from different species. Letters in bold on the top and bottom of the alignments represent invariant residues. Cys and His residues that constitute the putative zinc finger are boxed. Upward-pointing arrows indicate the Cys double mutant. The scheme in the middle summarizes our findings here. The cylinder and the grove represent RNAP domains involved in the front and rear DNA interactions, respectively. DNA chains are represented by open circles, and the RNA 3′ terminus is symbolized by a ball. The rest of the RNA is not shown. Abbreviations for the amino acid residues are as follows: A, Ala; C, Cys; D, Asp; E, Glu; F, Phe; G, Gly; H, His; I, Ile; K, Lys; L, Leu; M, Met; N, Asn; P, Pro; Q, Gln; R, Arg; S, Ser; T, Thr; V, Val; W, Trp; and Y, Tyr.

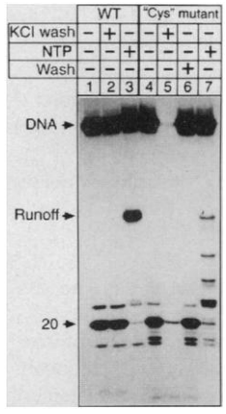

Fig. 8. Properties of the zinc finger ("Cys") mutant. The +20 starting complex formed with the wild-type (WT) or Cys mutant RNAP (*9*) was subjected to high salt concentrations (lanes 2 and 5) or allowed to extend RNA for 3 min in the chase reaction (lanes 3 and 7) containing NTPs at a concentration of 250 μM each. The ternary complex with a 20-nt transcript was prepared under conditions of RNAP excess over the template (lanes 1 and 4). Both the transcript and the template could be recovered from the carrier beads after washing with the low-salt buffer (lane 6). Under the same conditions of chase as in lane 7, the wild-type complex yielded the stoichiometric amount of the runoff transcript (lane 3).

residues that constitutes the zinc finger domain in many DNA binding proteins (8) (Fig. 7). The zinc finger motif is evolutionarily conserved, even though its position in prokaryotes and eukaryotes relative to other conserved amino acids is slightly different. To assess the functional significance of the zinc finger, we obtained a mutant in which the two conserved Cys residues were substituted with Ser. The Cys mutation was engineered in the *rpoC* expression plasmid pMKA201 carrying the His^6-fusion at the β' subunit COOH-terminus (9). The mutation had a recessive lethal phenotype: the mutant plasmid failed to complement a chromosomal *rpoC* amber mutation, yet upon induction in a wild-type host, the mutant β' polypeptide did not inhibit cell growth. Thus, sufficient amounts of the mutant RNAP could be recovered from the induced cells with the help of affinity chromatography on Ni^{2+} chelating agarose.

We compared the Cys mutant RNAP with the wild-type enzyme (Fig. 8). Ternary complex with a 20-nt transcript was prepared under conditions of RNAP excess over the template. The 20-nt mutant complex displayed stability under low-salt conditions because both the transcript and the template could be recovered from the carrier beads after washing with the low-salt buffer (lane 6). At low salt concentrations, the mutant complex was able to be chased, but most of it never reached the end of the template and produced instead a family of shorter RNA products that were spread throughout the transcribed region (lane 7); these products apparently reflect premature dissociation of RNAP. Under the same conditions of chase, the wild-type complex yielded the stoichiometric amount of the runoff transcript (lane 3). Upon exposure to the high-salt buffer, the mutant 20-nt complex quantitatively fell apart, whereas the wild-type complex remained intact (lanes 5 and 2, respectively). Thus, the Cys mutation renders the elongation complex extremely sensitive to salt and considerably less processive.

Functional topology of the elongation complex. These results delineate the principal structure-functional elements, both in DNA and the protein, that participate in the maintenance of the elongation complex. We demonstrate that key interactions occur in two distinct localities whose spatial orientation follows from the features of the minimal DNA template. The front (F) interaction takes place just ahead of the point at which the double helix forks out into the transcription bubble. The F interaction is of a nonionic nature because it is salt-resistant. It involves ~7 bp of DNA that are contacted by the zinc finger motif in the NH_2-terminus of the β' subunit (*10*). The F interaction is primarily responsible for RNAP processivity. However, it is not needed for proper orientation of the template, the primer, and the enzyme in the active center because short-distance RNA synthesis occurs even when the F interaction is destroyed.

The rear (R) interaction occurs immediately upstream from the DNA forking point and requires ~6 nt of the template strand of DNA, whereas the nontemplate strand is not involved. The R interaction is ionic because it is extremely salt-sensitive. It encompasses at least one untranscribed nucleotide ahead of the growing end of RNA and about five template nucleotides that have been transcribed. The 3′ terminus of RNA must be paired to at least two of the template DNA bases (*11*), so it is likely that the RNA tip participates in the R interaction. The R interaction may be simply a set of trilateral contacts between the template, the enzyme, and the product that constitutes the active center. In accordance with this suggestion, the crosslinking data pinpoint a 43–amino acid segment in the COOH-terminal region of β as the protein component of the R interaction. This region, between Met^{1230} and Met^{1273}, participates in the 5′ face of the catalytic pocket because His^{1237} crosslinks to the γ-phosphate of the priming NTP (*12*).

The delineation of F and R interactions allows one to envisage the trajectory of DNA in the elongation complex in terms of the global RNAP architecture. RNA polymerase subunits have a modular organization, whereby independently folded domains are connected by dispensable regions (Fig. 7). The Met^{1230}-Met^{1273} segment is a part of the well-characterized COOH-terminal domain of the β subunit (~300 amino acids) that folds and functions as a distinct entity (*13*). This domain can bind the priming NTP (*13*), which suggests that it holds the 3′ terminus of the RNA during elongation. Our results here indicate that the COOH-terminal domain of β also participates in the holding of the template DNA strand just behind the forking point.

The zinc finger motif of β′ that, according to our results, is involved in the F interaction is a part of the putative NH_2-terminal domain of β′ that encompasses approximately 600 residues between the terminus and the point where the sequence of the subunit is interrupted in chloroplasts (Fig. 7). Our results indicate that the COOH-terminal domain of β and the NH_2-terminal domain of β' are juxtaposed in the folded RNAP molecule in such a way that the Met^{1230}-Met^{1273} segment and the zinc finger face each other. The two protein sites must be in particularly close contact near position +6 relative to the RNA terminus, where both of them crosslink.

Thus, the trajectory of incoming DNA in the ternary complex passes first through the NH_2-terminal domain of β′; then, after DNA forks, the template strand enters a channel in the COOH-terminal domain of β that leads through the active center. It is tempting to speculate that movements of the two domains relative to each other have to do with the discontinuous elongation mechanism that follows from irregular DNA footprints of ternary complexes (*6*, *14*). However, our results here do not establish any relation between F and R interactions and the RNA polymerase elements deduced from the footprints (*6*).

Mechanism of elongation processivity. The classical model of transcription elongation attributes the critical role in the stability of the ternary complex to the strength of the RNA-DNA hybrid in the "transcription bubble." This model explains termination as the direct consequence of the weakness of the DNA-RNA hybrid (*15*). Our results here suggest on three counts that this model is not accurate. (i) The crucial salt-resistant interaction occurs downstream of the RNA growing point where no DNA-RNA hybrid exists. (ii) The upstream R interaction is very sensitive to salt concentration, an effect opposite the one expected for a DNA-RNA hybrid that should be stabilized by salt. (iii) A GC-rich sequence in the primary template that should produce a particularly stable hybrid appears to weaken the R interaction (Fig. 4).

On the other hand, our results are in agreement with previous reports on the effect of salt and the role of downstream sequences in the ternary complex (*16*). Thus, we favor the view that protein-DNA and protein-RNA interactions play a crucial role in the stability of the ternary complex, whereas the role of the DNA-RNA hybrid is minimal. This does not necessarily indicate that the hybrid is absent; it simply indicates that the hybrid does not have a direct role in the stability of the ternary complex.

To explain processivity, one can imagine a mechanism similar to that found in DNA polymerase where the conflict between strong template binding and unimpeded lateral movement is resolved with a ring-shaped "clamp" subunit (*17*). Recent structural comparison of the initiatory holoenzyme and elongation-competent core of *E. coli* RNAP suggests that a ring structure may be formed in the course of a major conformational transition at the time of promoter clearance (*18*). In the context of our results here, one can imagine that the transition would involve moving the NH_2-terminal domain of β′ close to the DNA so that the putative ringlike clamp locks around the DNA duplex just ahead of the transcription bubble.

We propose here a model of how such

conformational transition may be effected. We have shown previously that nascent RNA oligonucleotide entering the area just upstream of the active center causes the locking of RNAP on DNA in a salt-resistant complex (*19*). We now demonstrate that salt-resistant interactions between protein and DNA occur downstream of the RNA 3′ terminus. To reconcile these two observations, we suggest that the transcript channel leading out of the active center serves as an allosteric site for the locking of the downstream clamp. Filling the channel with nascent RNA triggers a conformational transition, which constitutes promoter clearance. During termination, the clamp must reopen in a reverse transition, whereby the zinc finger disengages from the DNA duplex. Again, this process can be effected allosterically by RNA leaving the upstream channel.

In a model of transcription elongation, Chamberlin and co-workers postulated that two RNAP sites alternately grip the template as the complex moves ahead (*11*). The notion of the bifunctional nature of the RNAP-DNA interaction agrees with the observation that the DNA replication complex can bypass the transcription elongation complex (*20*). This phenomenon is most easily explained by the existence of two alternating DNA binding sites in RNAP. By explaining processive elongation in terms of R and F interactions, our results provide a structural basis to this hitherto theoretical argument. Specifically, our model proposes that in the elongation complex DNA is held at two sites: the nonprocessive catalytic center in the COOH-terminal domain of β and the front-end lock that ensures processivity and involves the zinc finger of β′. The high evolutionary conservation of the RNA polymerase regions involved suggests that the proposed mechanism is of a general nature.

REFERENCES AND NOTES

1. T. D. Yager and P. H. von Hippel, in Escherichia coli *and* Salmonella typhimurium, *Cellular and Molecular Biology*, F. C. Neidhardt, Ed. (American Society for Microbiology, Washington, DC, 1987), pp. 1241–1275.
2. T. Platt, *Annu. Rev. Biochem.* **55**, 339 (1986); D. I. Friedman, M. J. Imperiale, S. Adhya, *Annu. Rev. Genet.* **21**, 453 (1987); J. W. Roberts, in *Transcription Regulation*, K. Yamamoto and S. McKnight, Eds. (Cold Spring Harbor Laboratory Press, Cold Spring Harbor, NY, 1992), pp. 389–406; A. Das, *Annu. Rev. Biochem.* **62**, 893 (1993); J. Greenblatt, J. R. Nodwell, S. W. Mason, *Nature* **364**, 401 (1993).
3. T. Aso, J. W. Conaway, R. C. Conaway, *FASEB J.* **9**, 1419 (1995); T. K. Kerppola and C. Kane, *ibid.* **5**, 2833 (1991).
4. G. Rhodes and M. J. Chamberlin, *J. Biol. Chem.* **249**, 6675 (1974); J. H. Roe, R. R. Burgess, M. T. Record Jr., *J. Mol. Biol.* **176**, 495 (1984).
5. M. Kashlev *et al.*, *Gene* **130**, 9 (1993).
6. E. Nudler, A. Goldfarb, M. Kashlev, *Science* **265**, 793 (1994).
7. M. A. Grachev *et al.*, *Eur. J. Biochem.* **180**, 577 (1989).
8. J. M. Berg and Y. Shi, *Science* **271**, 1081 (1996); I. Treich, M. Riva, A. Sentenac, *J. Biol. Chem.* **266**, 21971 (1991); D. P. Giedroc and J. E. Coleman *Biochemistry* **25**, 4969 (1986).
9. The Cys mutant (see Fig. 7) was engineered by M. Kashlev (unpublished result) in the β′ subunit expression plasmid pMKA201 (*5*) using standard techniques of oligonucleotide-directed mutagenesis. The Cys mutant was purified as described for His-tagged RNAP (*21*). The +20 ternary complex was prepared in a standard walking protocol (*22*). Five times molar excess of Cys RNAP over DNA template was reached to obtain the amount of +20 ternary complex that was comparable to the amount of the one containing wild-type RNAP.
10. It should be noted that mutations in this region have been shown to affect antitermination in bacteriophage HK022 [M. Clerget *et al.*, *J. Mol. Biol.* **248**, 768 (1995)].
11. G. A. Rice, C. M. Kane, M. J. Chamberlin, *Proc. Natl. Acad. Sci. U.S.A.* **88**, 4245 (1991); M. J. Chamberlin, *Harvey Lect.* **88**, 1 (1995).
12. A. Mustaev *et al.*, *J. Biol. Chem.* **268**, 19185 (1993).
13. K. Severinov *et al.*, *Proc. Natl. Acad. Sci. U.S.A.* **92**, 4591 (1995).
14. B. Krummel and M. J. Chamberlin, *J. Mol. Biol.* **225**, 239 (1992); D. Wang *et al.*, *Cell* **81**, 341 (1995); E. Nudler *et al.*, *ibid.*, p.353.
15. T. D. Yager and P. H. von Hippel, *Biochemistry* **30**, 1097 (1991); P. H. von Hippel and T. D. Yager, *Science* **255**, 809 (1992).
16. K. M. Arndt and M. J. Chamberlin, *J. Mol. Biol.* **213**, 79 (1990); A. P. W. Telesnitsky and M. J. Chamberlin, *ibid.* **225**, 239 (1992).
17. X.-P. Kong, R. Onrust, M. O'Donnell, J. Kurijan, *Cell* **69**, 425 (1992); T. S. R. Krishna *et al.*, *ibid.* **79**, 1233 (1994).
18. A. Polyakov, E. Severinova, S. A. Darst, *ibid.* **83**, 365 (1995).
19. S. Borukhov *et al.*, *J. Biol. Chem.* **268**, 23477 (1993); K. Severinov and A. Goldfarb, *ibid.* **269**, 31701 (1994).
20. B. Liu, M. L. Wong, R. L. Tinker, E. P. Geiduschek, B. M. Alberts, *Nature* **366**, 33 (1993).
21. His-tagged RNAP was purified by a modified procedure (*23*) from induced XL1-Blue cells carrying the pMKA201 plasmid (*5*). We resuspended ~6 g of cells in ~100 ml of buffer A [50 mM tris (pH 7.9); 5% glycerol; 2 mM EDTA; 0.1 mM dithiothreitol; 1 mM mercaptoethanol; 0.23 M NaCl; 130 μg/ml of lysozyme; and 40 μg/ml phenylmethylsulfonyl fluoride]. Sodium deoxycholate was added to a final concentration of 0.05%, and after 15 min at 4°C the suspension was passed through a French press. The cell debris was removed by centrifugation, and the protein material was precipitated with 0.35% Polymin P (BRL) (pH 7.9). The pellet was washed in five cycles of resuspension in ~150 ml of TGED [10 mM tris (pH 7.9); 5% glycerol; 1 mM EDTA; and 1 mM dithiothreitol] + 0.5 M NaCl and centrifugation. The material was extracted with 100 ml of TGED + 1 M NaCl, the pellet was discarded, and the supernatant material was precipitated with 2.5 volumes of saturated $(NH_4)_2(SO_4)$. The precipitate was dissolved in 20 ml of TGED, dialyzed, and purified on a 5-ml heparin-Sepharose column with a step-wash with 0.3 M NaCl and batch elution with 0.6 M NaCl in a TGED buffer system. The material was then batch-adsorbed to ~5 ml of Ni-NTA agarose (Qiagen) equilibrated with TGED for at least 1 hour with gentle mixing; the beads were washed three times by centrifugation and resuspension in ~30 ml of TGED + 1 M NaCl and two times in TGED. RNAP was batch-eluted with ~10 ml of TGED + 100 mM imidazole + 0.3 M NaCl for at least 1 hour. After removal of the beads by centrifugation, the supernatant was concentrated to ~500 μl, fractionated on a Superose 6 10/30 FPLC (Pharmacia) column, and further purified by chromatography on an FPLC MonoQ 5/5 column.
22. In the reaction for 10 samples, 2 pmol (1 μl) of His-tagged RNAP (*21*), 1 pmol (1 μl) of T7A1 promoter DNA template fragment (*24*), and 6 μl of TB [50 mM tris-HCl (pH 7.9), 10 mM $MgCl_2$, and 100 mM KCl] were incubated for 5 min at 37°C. We added 5 μl of TB–pre-equilibrated Ni-NTA agarose beads (Qiagen) and incubated them for 10 min. We added 2 μl of the starting cocktail to give the final concentration of CpApUpC primer of 20 μM and of 25 μM for both ATP and GTP. After 4 min at 37°C, the beads were washed four times with 1.5 ml of TB, resuspended in 10 μl of TB containing 0.3 μM [α-^{32}P]cytidine triphosphate (3000 Ci/mmol), and incubated for 5 min at room temperature. The beads were washed four times and resuspended in 10 μl of TB containing 0.3 μM [γ-^{32}P]ATP (>3000 Ci/mmol) and incubated for 10 min at room temperature with 1 μl (10 units) of polynucleotide kinase (New England Biolabs). To obtain the +34 complex, we performed three successive walking reactions (ATP+CTP+GTP, ATP+UTP+GTP, and CTP+ATP+UTP) in 50 μl of TB and NTPs (5 μM each) for 3 min at room temperature; the reactions were interrupted each time with four cycles of centrifugation and resuspension in 1.5 ml of TB. The beads were then transferred into the low-salt TB [50 mM tris HCl (pH 7.9); 10 mM $MgCl_2$; and 5 mM KCl], and the suspension was aliquoted according to the experimental protocol of Fig. 1 so that the final volume of each single reaction would be 10 μl. Where indicated in Fig. 1, the secondary template was added in a 100-fold molar excess over RNA polymerase. NTPs in the chase reactions (1 min at room temperature) were at a concentration of 250 μM each. The high-salt wash (0.5 M KCl in TB) was for 30 s followed by centrifugation and resuspension in the standard TB. Where indicated, the secondary template was end-labeled with [γ-^{32}P]ATP as described above in the template oligonucleotide. The kinase was inactivated by heating for 1 min at 90°C before annealing with the complementary strand (*24*).
23. R. R. Burgess and J. J. Jendrisak, *Biochemistry* **14**, 4634 (1975).
24. The two promoter-containing templates (Fig. 1) were obtained by polymerase chain reaction (PCR) from the pENtR2 plasmid (E. Nudler, unpublished results). The sequence of the primary template is as follows: TCCATCCAGA TCCCGAAAAT TTATCAAAAA GAGTATTGAC TTAAAGTCTA ACCTATAGGA TACTTACAGC CATCGAGAGG GACACGGCGA ATAGCCATCC CAATCGACAC CCCGGGAAAA (the transcribed sequence is underlined). The secondary templates were obtained from Oligos, Inc. For 10 reaction samples, 100 pmol each of the "top" and "bottom" strand oligonucleotides (*22*) were mixed in a volume of 10 μl in the low-salt TB, heated for 30 s at 90°C in a PCR machine, and then allowed to slowly cool to room temperature while remaining in the heating block. The material was then diluted to one-tenth its original concentration into the transcription reaction.
25. V. Markovtsov *et al.*, *Proc. Natl. Acad. Sci. U.S.A.* **93**, 3231 (1996).
26. For 10 reactions, the +20 ternary complex was prepared in a standard walking protocol (*22*) and was treated with 10 units of exonuclease III (ExoIII; New England Biolabs) for 10 min at room temperature. ExoIII was removed by two rounds of washing of the RNAP beads (once in high-salt buffer and once in standard TB). The material was treated with Sma I restriction endonuclease (New England Biolabs, 20 units, 10 min at room temperature), and the complex was walked to the desired positions.
27. The derivatized template oligonucleotide was custom-synthesized (Oligos Etc.) and was end-labeled with polynucleotide kinase. The +55 switchover complex was prepared (*22*) and exposed to UV (308 nm, 6 W Cole Parmer 9815 lamp placed on top of an Eppendorf tube for 20 min) and processed for electrophoresis as described (*25*).
28. G. Puhler *et al.*, *Proc. Natl. Acad. Sci. U.S.A.* **86**, 4569 (1989); D. Sweetser, M. Nonet, R. A. Young, *ibid.* **84**, 1192 (1987).
29. K. J. Bergsland and R. Haselkorn, *J. Bacteriol.* **173**, 3446 (1991).

30. We are grateful to A. Mustaev for advice on crosslinking techniques and to M. Kashlev for providing the Cys *rpoC* mutant. This work was supported by NIH grant GM49242. E.A. is in the graduate program of the Institute of Molecular Genetics, Russian Academy of Sciences.

11 April 1996; accepted 30 May 1996